I&EC research
Industrial & Engineering Chemistry Research

Article

pubs.acs.org/IECR

Influence of Peroxynitrite in Gliding Arc Discharge Treatment of Alizarin Red S and Postdischarge Effects

D. R. Merouani,[†] F. Abdelmalek,*[,†] M. R. Ghezzar,[†] A. Semmoud,[‡] A. Addou,[†] and J. L. Brisset[§]

[†]Laboratoire des Sciences et Techniques de l'Environnement et de la Valorisation (STEVA), Faculté des sciences et de la technologie, Université de Mostaganem, 27000, Mostaganem, Algérie

[‡]Laboratoire de Spectrochimie Infrarouge et Raman (LASIR), Université des Sciences et Technologies de Lille, 59650 Villeneuve d'Ascq, France

[§]Faculté des Sciences, Université de Rouen, Mont-Saint-Aignan, France

ABSTRACT: The gliding arc discharge is a cheap and efficient nonthermal plasma technique able to degrade organic compounds dispersed in water at atmospheric pressure. Alizarin Red Sulfonate (ARS) is selected as a stable quinonic dye. Exposure of the dye solution to the discharge in a batch reactor induces two successive reaction steps according to the treatment conditions. Direct exposure of the solution to the discharge induces simultaneous bleaching and COD evolution. In postdischarge conditions, that is, after the discharge is switched off, the reactions keep on developing. This study thus underlines two key features: the ability of glidarc discharges to degrade recalcitrant molecules and the low cost of the process which requires short exposure times. A model mechanism involves peroxynitrite as a likely active species formed in the discharge and involved in postdischarge phenomena in aqueous solutions and suggests short exposure times and much longer postdischarge times for optimized pollutant abatement.

1. INTRODUCTION

Aqueous effluents from textile industries carry away numerous molecules belonging to various families of dyes (e.g., azo, quinonic, etc.) which may be difficult and expensive to degrade.[1] Anthraquinonic dyes are involved in polyamide, leather, and wool dyeing[2,3] and therefore are the most important ones after azo dyes for commercial reasons. They are classified as recalcitrant compounds which remain in aquatic ecosystems,[4,5] and their degradation is considered in several papers.[6−8] Alizarin Red Sulfonate (ARS) is an anthracene-like synthetic dye. It has a three-ring aromatic structure in the central part of it molecule plus various substituents.[9] It is widely used in the textile industry and for histochemical analyses[10,11] so that new techniques have to be proposed for its degradation.

The usual techniques[12] for treating liquid wastewaters, such as coagulation/flocculation, adsorption and biodegradation, activated carbon, reverse osmosis, ultrafiltration, etc., are not well adapted to this family of dyes, because of the high number of benzene ring which stabilize the molecule.[13,14] More efficient and less energy consuming processes must be developed to eliminate these pollutants or lower their harmful character. The newly developed advanced oxidation processes (AOPs) generate active hydroxyl radicals •OH which are claimed to degrade numerous organic compounds.[15−17] Some nonthermal plasma techniques, such as corona,[18,19] dielectric barrier discharge (DBD),[20] or gliding arc discharges (GAD) belong to these AOPs: they burn at atmospheric pressure in conditions halfway from thermal and nonthermal plasmas, since electrons and heavy particles are not fully thermalized as they are in thermal plasmas. Thus the macroscopic temperature remains close to room. The GAD is actually "quenched" plasma with a composition close to a thermal plasma and therefore a thermal effect of only few degrees. Compared with other plasma techniques, the GAD is considered as a promising technique well adapted to the pollutant abatement of aqueous effluents, and several examples relevant to the elimination of biorecalcitrant organic compounds found in domestic and industrial wastewaters illustrate this assertion: (i) degradation of various dyes, for example, azo dyes such as Orange II, yellow supranol 4 GL, Red Nylosane F3 GL, Eryochrome Black T, Orange G, Methylorange; triphenylmethane dyes such as Malachite Green, Crystal Violet, Bromothymol Blue; and anthraquinonic dyes such as Acid Green 25, ARS;[5,21−26] (ii) degradation of polymers rejected by industry,[27] degradation of two polluted textile wastewaters[28] eliminating organic waste solutes,[29] destruction of nicotine;[30] (iii) mineralization of the tributylphosphate present in the nuclear industry rejects;[31] trilaurylamine for nuclear industry processes[32] degradation of phenol,[33] Bisphenol A in solution.[34]

The gliding arc discharge involves higher quantities of energy than other cold discharges at atmospheric pressure and thus presents several advantages; for example, it generates a larger population of active species, without the need of incorporated reagent and mainly favors the occurrence of postdischarge phenomena (i.e., a self-development of the chemical reactions in the solution after the discharge is switched off) which are of significant interest for industrial applications by lowering the running cost of the process.

The GAD treatment of aqueous solutions consists of exposing the target solution to the discharge burning in air over the liquid in a batch or a circulating reactor. The discharge

Received: October 31, 2012
Revised: December 12, 2012
Accepted: December 24, 2012
Published: December 24, 2012

dx.doi.org/10.1021/ie302964a | *Ind. Eng. Chem. Res.* 2013, 52, 1471−1480

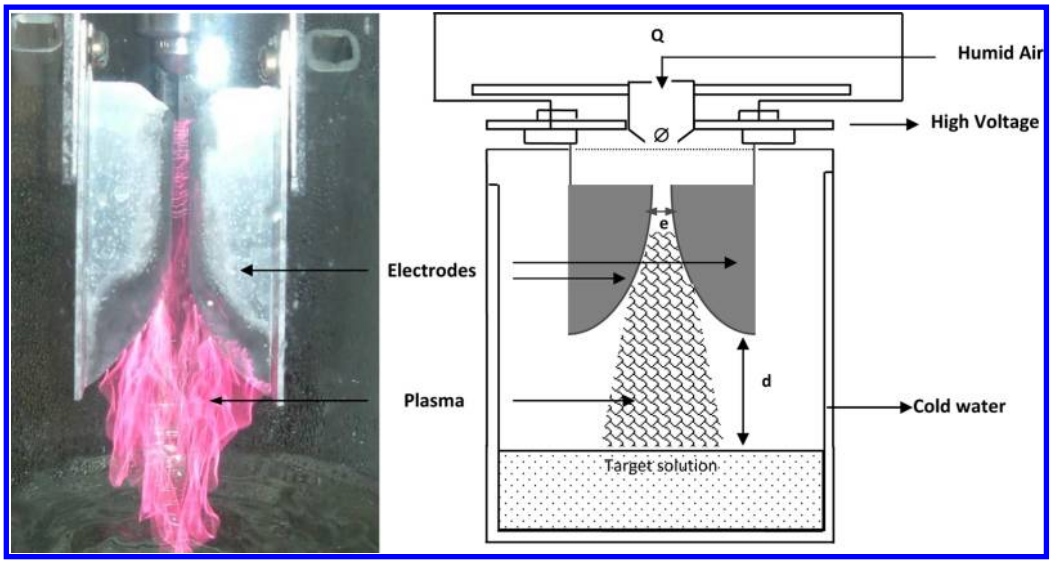

Figure 1. Experimental setup of the gliding arc plasma device with humid air feeding gas. The pink color of the plasma cloud is due to oxygen.

generates an active oxidizing species; some of them are long life water-soluble moieties and are responsible for temporal postdischarge reactions (TPDR) which develop in the liquid phase.[35]

Several examples of TPDR are reported in the literature, for example, as follows: (i) The gliding arc oxidation of ferrous to ferric ions develops in two steps. The first step is rapid, associated with the exposure time to the discharge and would be attributed to $^{\bullet}OH$ at the liquid surface; the second step is a slow TPDR, due to H_2O_2 and other dissolved species.[36] (ii) TPDR was also evidenced for nucleophilic substitutions by corona discharge treatment in CO.[37] (iii) Bacterial inactivation in postdischarge conditions;[38] the authors underline the economical advantage of the plasmachemical bacterial inactivation without extra energy or reagent input. (iv) Moussa et al.[35] evidenced TPDR in the plasmachemical treatment of methyl orange and attribute the degradation to the species H_2O_2 and HNO_2 formed in the discharge. (v) Brisset et al.[39] considered the influence of peroxynitrite $ONOO^-$ and its matching acid which are soluble in water, able to dissociate into $^{\bullet}OH$ and ONO^- and to induce oxidizing, nitrating, and nitrosing postdischarge effects on solutes. (vi) The GAD treatment of surface waters[40] induced an increase in the BOD abatement after switching off the discharge, and this feature was attributed to the oxidizing power of peroxynitrous acid ONOOH. The formation of transient nitrite ions was evidenced which is the source of peroxynitrite $ONOO^-$, i.e., a transient precursor to nitrate,[41] according to the following sequence:

$$N_2 \rightarrow NO_2^- \rightarrow ONOO^- \rightarrow [NO_3^- + H^+] \quad (1)$$

The GAD (or glidarc) was first proposed by Lesueur et al.[42] and developed by Czernichowski[43] for the decontamination of gases. The technique is based on the production of quenched nonthermal plasma generated by an electrical arc often burning in air. The efficacy of the treatment results from the presence in the plasma cloud of active chemical species, radicals, excited molecules, and ions, such as $^{\bullet}OH$, $^{\bullet}NO$, $O^{\bullet}$, O_2, $HO_2^{\bullet}$, $H^{\bullet}$, H_2O_2, O_3, O_2^+, N_2^+, O^+, N^+, etc. The most reactive species are the hydroxyl radicals $^{\bullet}OH$ due to their high standard oxidation potential $E^{\circ}(^{\bullet}OH/H_2O)$ = 2.8 V/SHE which is among the strongest known oxidizing potentials. Emission spectra analysis[44] of the gliding arc discharge in humid air shows the occurrence of $^{\bullet}OH$ and $^{\bullet}NO$, and allows quantifying the population of the formed species. $^{\bullet}OH$ results from the dissociation of water molecules by electron (or/and photon) impact, while the endothermal formation of $^{\bullet}NO$ (according to the Birkeland process) requires the occurrence of an electric arc. The main relevant reactions are given below (reactions 2−7):

$$H_2O + \bar{e}(\text{or } h\nu) \rightarrow H^{\bullet} + {}^{\bullet}OH + \bar{e} \quad (2)$$

$$2H_2O + \bar{e} \rightarrow H_2O_2 + H_2 + \bar{e} \quad (3)$$

$$O_2 + \bar{e}\ (+M) \rightarrow 2O^{\bullet} + \bar{e}\ (+M) \quad (4)$$

$$N_2 + O^{\bullet} \rightarrow {}^{\bullet}NO + N^{\bullet} \quad (5)$$

$$N^{\bullet} + O^{\bullet} \rightarrow {}^{\bullet}NO \quad (6)$$

$$N^{\bullet}(^2D) + O_2 \rightarrow {}^{\bullet}NO + O^{\bullet} \quad (7)$$

The hydroxyl radical and nitric oxide are the precursors of derivatives that react at the liquid surface and/or in the solution provided they are soluble.

This work is devoted to the systematic investigation of the behavior of an anthraquinonic dye (ARS) under discharge and, for the first time, postdischarge conditions. Peroxynitrite ($ONOO^-$), that is, oxoperoxonitrate(−1) according to the official quoting, is a derivative of NO and NO_2 formed at the liquid surface, soluble in water, and the precursor of isomer forming reaction yielding nitric acid. This active specie formed in the discharge is involved in postdischarge phenomena in aqueous solutions.

The matching acid ONOOH is weak (pK_a = 6.8) but granted with strong oxidizing properties ($E^{\circ}(ONO_2H/NO_2)$) = 2.02 V/SHE. The acid−base system is involved in discharge and postdischarge reactions.[35,39,45]

2. MATERIALS AND METHODS

2.1. Reagents and Plasma-Reactor. Alizarine Red Sulfonate, ARS ($C_{14}H_7NaO_7S$, also referred to as 1,2-dihydroxy-9,10-anthraquinonesulfonic acid sodium salt or Mordant Red 3; C.I. 58005; molecular weight: 342.28g) is a

dx.doi.org/10.1021/ie302964a | Ind. Eng. Chem. Res. 2013, 52, 1471−1480

commercial dye (analytical grade) purchased from Acro Organics.

Distilled water was used to prepare dye solutions of suitable concentration. ARS is a triacid of H_3I type: the first acidity is strong; the two others are medium or weak pK_a (H_2I^-/HI^{2-}) = 5.5 and pK_a(HI^{2-}/I^{3-}) = 10.8. The relevant colors are colorless (H_3I), yellow (H_2I^-), red (HI^{2-}) and purple (I^{3-}). Natural ASR solutions absorb at 430 nm and their pH is 6.5.

The experimental apparatus of the GAD used is shown in Figure 1. Compressed gas is led through a bubbling water flask to get water-saturated. The gas flow then passes between two semielliptic electrodes connected to a 220 V/9 kV high voltage Aupem Sefli transformer. It produces an alternative potential difference of 9000 V and a current intensity of 100 mA in open (and 600 V/160 mA in working) conditions. The delivered power is close to 100 W, which considerably lowers the running cost of the process.

An electrical arc forms between two diverging electrodes raised to a convenient voltage difference at the minimum gap. The arc is pushed away from the ignition point by the feeding gas flow and sweeps along the electrodes to the maximum electrode gap where it breaks into a large plasma plume. A new arc then appears and develops according to the same procedure. The length of the electric channel increases so that the plasma temperature falls before breaking. The resulting plasma is actually a quenched plasma at atmospheric pressure and quasi-ambient temperature. The diffusion process in the liquid is improved by conversion in the liquid phase due to the airflow and magnetic stirring.

The treatment is performed in batch mode with the working parameters: the gas flow is fixed at Q = 700 L h^{-1}, the electrode gap e = 2 mm, the nozzle diameter is 1 mm, and the distance between the electrodes and the liquid surface d = 3 cm. The solution temperature is thermostatted at 20 ± 2 °C by circulating water in a jacket.

2.2. Plasma Treatments of ARS Samples. *2.2.1. Direct Exposure of ARS Solutions to the Discharge.* ARS aqueous samples (100 and 335 μM) were poured in the 500 mL pyrex vessel. The evolution of the treatment of the dye solution under plasma treatment in batch mode was followed for various exposure times t^* (0, 10, 20, 30, 60 min) and analyzed immediately after sampling ("snapshot analysis").

2.2.2. Postdischarge Experiments. The sample solutions were exposed to the discharge in the same conditions as for direct exposure experiments, that is, for t^* = 1, 2, 5, 10, 15, 30, and 60 min before being abandoned outside the reactor for various postdischarge times t_{TPDR} before the analyses were performed. A preliminary set of experiments was performed on 100 μM ARS solutions and involved t_{TPDR} = 0.25, 0.5,1, 2, 3, 4, 5, 6, and 24 h postdischarge delays. The second set of experiments concerned 335 μM ARS solutions and longer postdischarge times: t_{TPDR} = 1, 2, 3, 5, 10, 24, 48 h, 5, 7, and 30 days.

Analyses were performed by measuring absorbance A at 430 nm (with Optizen UV−vis spectrophotometer) and COD by the potassium dichromate standard method.[46] COD and bleaching rates were calculated as follows:

$$\text{degradation (\%)} = \frac{(\text{COD}_0 - \text{COD}_i)}{\text{COD}_0}100$$

where COD_0 and COD_i refer to the COD values before and after treatment, respectively, and

$$\text{bleaching (\%)} = \frac{(A_0 - A_i)}{A_0}100$$

Where A is the absorbance value at the absorbance peak in the visible wavelength range; A_0 and A_i are the absorbance values before and after treatment, respectively.

3. RESULTS AND DISCUSSION

3.1. Preliminary Treatment: Direct Exposure of ARS to the Glidarc. *3.1.1. Diffusion of Active Species in the Solution: Effects of pH and Conductivity.* Exposing ARS (100 μM) solutions to the discharge in humid air induces increases in acidity and matching conductivity. pH falls from 6.5 to 3.5 within 1 min and trends to 1.55 for 1 h exposure time while conductivity increases from 20 to 5290 μS cm^{-1} for t^* = 1 h.

Analyses of distilled water exposed to the discharge in the same conditions evidenced the formation of nitrite and nitrate up to 202 and 607 mg L^{-1}, respectively.

Humid air plasma treatment of solutions involves that formed active species are water-soluble enough to enter the solution and get dissolved, in particular, H_3O^+, NO_2^-, and NO_3^- which are involved in the pH lowering process via the formation of nitrous and nitric acids (reactions 12−14).[47] A reaction scheme was recently proposed (reactions 8−15).[48]

$$^{\bullet}NO + {}^{\bullet}OH \rightarrow ONOH \quad (8)$$

$$NO + O \rightarrow ONO \quad (9)$$

$$ONO + NO + H_2O \rightarrow 2ONOH \quad (10)$$

$$NO^{\bullet} + HO_2^{\bullet} \rightarrow ONOOH \quad (11)$$

$$HNO_2 + H_2O_2 \rightarrow HNO_3 + H_2O \quad (12)$$

$$NO_2 + {}^{\bullet}OH \rightarrow H^+ + NO_3^- \quad (13)$$

$$ONOOH \rightarrow NO_3^- + H^+ \quad (14)$$

$$3NO_2^- + 2H^+ \rightarrow NO_3^- + 2NO + H_2O \quad (15)$$

The charge balance was not observed in most experiments[49−51] which consider only protons and nitrate ions after direct exposure and must be completed. For example for 1 h postdischarge, pH is measured as 1.55, which means C_{H^+} = 10^{-pH} = 28.2 mM and the resulting molar conductivity is:

$$\lambda_{H^+} \times C_{H^+} = 349.8 \times 28.2 = 9.86 \text{ mS cm}^{-1}$$

that is, a value higher than the measured conductivity of the solution, 5.23 mS cm^{-1}, which involves the conductivities of all the identified anions, such as nitrite and nitrate, whose molar conductivities are both close to 71.4 S mol^{-1} cm^2.

3.1.2. Influence of the Reactive Nitrogen Species (RNS) on ARS Bleaching. This work aims to underline the determining influence of nitrogen containing species (or Reactive Nitrogen Species), such as nitrite ONO^-, peroxynitrite $ONOO^-$, and nitrate NO_3^- in the bleaching process of ARS. The structure of peroxynitrite is linear, isomeric of nitrate, and a transient intermediate in the oxidation of nitrite to nitrate.[35,45]

Previously published works on $ONOO^-$ synthesis gather the reactions involving NO_2^-, NO_3^- and oxygen donor species, such as O, O_3, H_2O_2, etc.[52] Starting from either NO_2 or NO_2^-:

$$O + NO_2^- \rightarrow ONOO^- \quad (16)$$

dx.doi.org/10.1021/ie302964a | Ind. Eng. Chem. Res. 2013, 52, 1471−1480

Table 1. Bleaching of ARS Directly Exposed to the Gliding Discharge in Air, with and without Sulphamic Acid (SA)

	$\%R_{bleaching}$									
time t^* (min):	0	0.5	1	2	3	5	15	30	45	60
without SA	0.00	0	3.5	6.7	9.5	11.5	22.4	41.0	53.4	67.2
with SA	0	0	0	0	0	0	0.6	3.3	4.7	73

Table 2. Bleaching Ratio of 100 mM ARS Solutions Exposed for t^* (min) to the Discharge without and with (*bold italics*) Incorporated SA

		$\%R_{bleaching}$											
t_{TPDR} (min)	t^* (min):	0	***0***	1	***1***	2	***2***	3	***3***	5	***5***	15	***15***
0		0.00	0	3.52	0.00	6.74	0.00	9.54	0.00	11.52	0.00	22.37	0.61
15		0.00	0	3.96	0.00	7.39	0.00	10.20	0.00	12.61	0.00	24.34	0.61
30		0.00	0	4.18	0.00	10.65	0.00	16.05	0.00	17.39	0.00	31.58	0.61
60		1.09	0	7.25	0.00	16.52	0.00	20.61	0.00	28.70	0.00	38.60	1.84
120		1.31	0	15.82	0.00	26.30	0.00	29.93	0.00	33.26	0.83	45.39	3.47
180		1.53	0	35.60	0.00	35.00	0.00	38.18	0.00	41.30	1.03	45.39	3.67
240		2.18	0	36.70	0.00	42.17	0.00	45.34	0.41	50.87	1.86	51.75	4.08
300		3.06	0	36.70	0.00	49.57	0.62	51.41	1.03	52.39	1.86	55.92	4.29
360		3.28	0	44.62	0.00	50.87	0.62	53.15	1.24	53.26	1.86	62.94	4.29
1440		3.93	0	81.54	0.83	85.65	1.65	86.98	2.06	87.83	2.89	88.82	4.29

$$O^{\bullet -} + ONO^{\bullet} \rightarrow ONOO^{-} \quad (17)$$

$$ONOOH \leftrightarrow ONOO^{-} + H^{+} \quad (18)$$

$$O_2^{-\bullet} + {}^{\bullet}NO \rightarrow ONOO^{-} \quad (19)$$

or from NO_3^-[53]

$$e_{aq}^{-} + NO_3^{-} \rightarrow NO_3^{\bullet 2-} \quad (20)$$

$$NO_3^{\bullet 2-} + H_2O \rightarrow NO_2 + 2OH^{-} \quad (21)$$

$$^{\bullet}OH + NO_2 \rightarrow ONOOH \quad (22)$$

$$ONOOH \leftrightarrow H^{+} + ONOO^{-} \quad (23)$$

We can incidentally point out that nitrite anions are thermodynamically unstable for pH < 6, due to the disproportionation of NO_2^- into NO_3^- and NO:

$$3NO_2^{-} + 2H^{+} \rightarrow NO_3^{-} + 2NO + H_2O \quad (24)$$

as considered elsewhere.[39,48]

A clear evidence of the essential role of the RNS in ARS bleaching process results from treatments of the dye with and without a reducer of the nitrites,[54] such as sulphamic acid NH_2SO_3H according to

$$HNO_2(l) + NH_2SO_3H(l) \rightarrow N_2(g) + H_2SO_4(l) + H_2O(l) \quad (25)$$

which shows that nitrous acid is reduced into nitrogen. Thus incorporating sulphamic acid (SA) to the reactor prevents nitrite and RNS formation; it remains to check the changes induced in solution by the plasma treatment and to compare the results with and without NH_2SO_3H.

We thus achieved two sets of plasma treatments of ARS with and without SA. The relevant results (Table 1) show bleaching rates of 53.4% and 4.7% with and without sulphamic quencher respectively for t^* = 45 min exposure. For longer t^* exposures (e.g., 1 h or longer), the bleaching rates are not largely different (67.2% and 73%, respectively). Such results are apparently conflicting but they can however be simply explained: incorporating an excess of sulphamic acid at the beginning of the treatment allowed for a reduction of all the nitrites already formed. For long exposure times the incorporated NH_2SO_3H molecules are no longer in excess because of their action on nitrite ions or because they have been degraded by the plasma formed oxidizers.

Iya-sou et al.[55] recently considered the action of long life species such as nitrogen oxides "formed over the solution by a gliding arc discharge in air in the degradation of model pollutants as phenol in direct exposure mode and in postdischarge conditions". In the case of moderately soluble phenol, the authors assume that the main mechanism for removal involves the action of $^{\bullet}NO_2$ radicals formed in the liquid phase from the dissociation of soluble N_2O_4. Unfortunately no author has detected $^{\bullet}NO_2$ or its dimer in the gas phase, $^{\bullet}NO$ readily oxidized to $^{\bullet}NO_2$ by numerous oxygen donor species, as mentioned above. Also, $^{\bullet}NO_2$ easily fixes an electron $E'^{\circ}(^{\bullet}NO_2/NO_2^-)$ = 0.99 V/SHE at pH 7 (i.e., in an acidity range where the nitrite ion is thermodynamically unstable). It may be incidentally pointed out that nitronium ion NO_2^+ and nitrosonium NO^+ are the oxidized forms of $^{\bullet}NO_2$ and $^{\bullet}NO$, respectively: [$E^{\circ}(NO_2^+/^{\bullet}NO_2)$ = 1.6 V/SHE and $E^{\circ}(NO^+/^{\bullet}NO)$ = 1.21 V/SHE] and are probably present in limited concentrations in the discharge cloud.

However, it is likely that among the RNS, peroxynitrite is one of the most efficient ones, due to its ability to react both as a strong oxidizer and as a source of nitrating/nitrosing agent. In the case of ARS degradation, the influence of RNS is essential.

Direct exposure of organic compounds to humid air plasma in batch conditions usually requires long treatment times. To save time and energy, the direct exposure time t^* was deliberately shortened in the scope of our investigation of TPDR.

3.1.3. Postdischarge Degradation of ARS (100 μM) in the Presence and Absence of Sulphamic Acid SA. This part of the study is devoted to show evidence of the determining role of the plasma generated RNS in the degradation of the dye with special emphasize on peroxynitrite[35,39] since the short lifetime of $^{\bullet}OH$ (few hundred nanoseconds) discards them from direct occurrence in the bleaching postdischarge process.[56]

dx.doi.org/10.1021/ie302964a | Ind. Eng. Chem. Res. 2013, 52, 1471−1480

A set of 16 ARS (100 μM) solutions were prepared and exposed to the glidarc in humid air for t^* (1, 2, 5, 10, 15, 30, 45, and 60) min with or without incorporated SA. After each exposure, the samples are disposed outside the plasma reactor and abandoned for various t_{TPDR} times in postdischarge conditions before being analyzed for absorbance and COD. The results for standard postdischarge times t_{TPDR} (0.25, 0.5, 1, 2, 3, 4, 5, 6, and 24 h) are gathered in Table 2.

Direct exposures to the discharge of samples without SA (e.g., for t^* = 1 and 15 min) induce bleaching rates by 3.52 and 22.37%; postdischarge on the same samples largely increases the ratio values bleaching (e.g., 36.7 and 51.75 for t_{TPDR} = 4 h and 81.54 and 88.82% for 24 h postdischarge. Conversely, bleaching remained negligible for samples with incorporated SA and exposed to the discharge in the same conditions.

For longer exposure times t^* (e.g., 30 and 60 min), the instant R values were 41 and 73% with and without SA, respectively. Postdischarge effects lead to respective abatements of 60.96 and 79.46% within 4 h and 89 and 91.55% for t_{TPDR} = 24 h postdischarge. The bleaching plasma treatment is almost inefficacious for short exposure times t^* in the presence of SA.

These results underline the efficacy of the TPDR which keep developing after the discharge is switched off, especially for short exposure times t^* (t^* < 15 min). They also evidence that some RNS, such as nitrite (and/or their derivative peroxynitrite) are responsible for postdischarge effects since SA affects the formation of nitrites. Such an assessment confirms previous studies on the glidarc degradation of methyl orange, orange G, and bisphenol A.[26,34,35]

The occurrence of TPDR reactions is now clearly confirmed. We have now to consider the relevant kinetics by means of absorbance and COD measurements. The influence of the starting ARS concentration is examined, and C (ARS) was increased up to 335 μM, as well as the postdischarge duration t_{TPDR} to 5, 7, and 30 days.

3.1.4. Bleaching and Degradation Kinetics of ARS by Direct Exposure to the Discharge. The absorbance spectrum of Alizarin Red S before treatment (Figure 2) is characterized

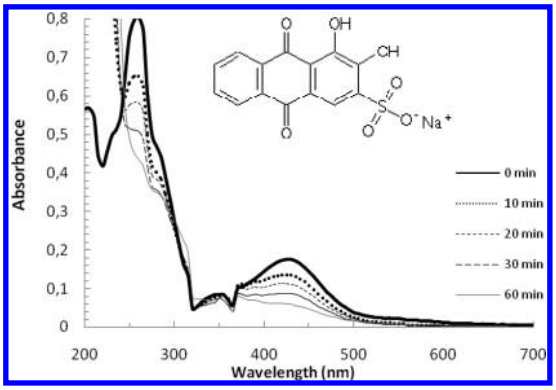

Figure 2. Instantaneous spectral evolution of a plasma-treated (335 mM) ARS aqueous solution exposed to the discharge: UV–vis absorption spectra and structure of untreated ARS dye.

by a band in the visible region with a peak at 430 nm which characterizes the chromophore group and two bands located at 260 and 345 nm which are attributed to the benzene rings substituted by SO_3^{2-} groups[26] and to the anthraquinonic part.

The absorbance at 260 nm decreases rather slowly and illustrates the progressive degradation of the anthracene ring. The spectral changes are probably relevant to the probable formation of intermediates on the benzene rings.[1] Direct exposure of 335 mM ARS solutions (Figure 3) to the plasma

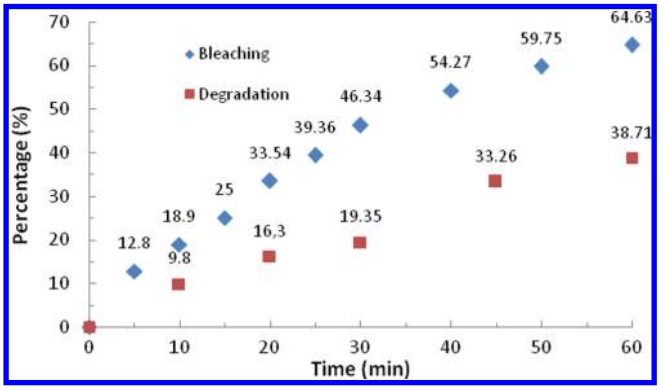

Figure 3. Evolution of bleaching (diamonds) and COD (squares) of 335 mM ARS solutions directly exposed to the discharge.

showed spectral abatements ("bleaching") of 46.3 and 64.6 for t^* = 30 and 60 min and the matching COD abatements ("degradation") are 19.7 and 38.7%, respectively. The evolution of COD with t^* follows a pseudo-first-order kinetic: $d[COD]/dt^* = -k[COD]$ or the integral form $\ln(C_0/C) = k_1 t^*$. The relevant kinetic constants for bleaching and degradation are respectively 0.0146 min^{-1} (R^2 = 0.983) and 0.008 min^{-1} (R^2 = 0.998).

According to the work of Jing Xue et al.,[20] the degradation process of AR in the hybrid gas–liquid dielectric barrier discharge (DBD) plasma can be divided into three phases: (a) gas-discharge phase; (b) ring-opening phase; (c) mineralization phase. A careless comparison of these results with ours is hazardous because our work was performed with a largely more powerful discharge involving arc which favored NO production. In particular there is probably no NO_x generated in DBDs, and hence, no peroxynitrite may be involved. Although this case is out of the scope of this work to examine in details the DBD study. It is likely that kinetic steps mentioned by Jing Xue et al. simultaneously develop in the case of glidarc discharges, as (^{31}P) NMR studies on the degradation of tributylphosphate suggest the occurrence of intermediates. Anyway we agree with the limited efficacy of the DBD process in the present case. Also, TPDR were not yet evidenced in the case of DBD. This is a substantial advantage of the glidarc technique, and an indirect argument in favor of the occurrence of peroxynitrite in the glidarc degradation processes.

3.2. Bleaching and Degradation of ARS in Postdischarge Conditions. The bleaching and degradation rates resulting from direct exposure of ARS solutions to the discharge for ARS are limited, for example $R_{bleaching}$ = 5, 7, and 19.3% and $R_{degradation}$ = 0, 4.6, and 19.3% for t^* = 1, 5, and 15 min direct exposure time. These samples were abandoned in postdischarge conditions for 48 h and 7 days. The matching abatements are gathered in Table 3 for illustration.

GAD treatment allows the acquisition of a bleaching and degradation rate that increases in function to t duration. However, in postdischarge, elimination rates give a maximum in 0 < t^* < 10 min interval and then decreases after this time (Figures 4 and 5). We have also noticed that elimination rates become significant from 10 h of postdischarge where the bleaching and degradation rates exceed 50%.

This feature may be interpreted on the basis of the assumption of the incorporation of a given amount of reactive

dx.doi.org/10.1021/ie302964a | Ind. Eng. Chem. Res. 2013, 52, 1471–1480

Table 3. Examples of Bleaching and Degradation Rates for Various Exposure Times t^*

	t^* (min) = 1		t^* (min) = 5		t^* (min) = 15	
t_{TPDR}	$\%R_{bleaching}$	$\%R_{degradation}$	$\%R_{bleaching}$	$\%R_{degradation}$	$\%R_{bleaching}$	$\%R_{degradation}$
t_{TPDR}, 0 min	5	0	7	4.6	19.3	19.3
t_{TPDR}, 48 h	66.6	36.1	82.1	59.5	57.3	42.6
t_{TPDR}, 7 days	80.7	51.1	87.3	66.7	60.9	43.7

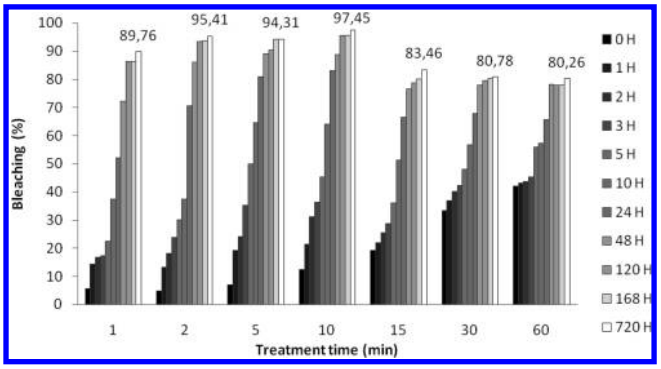

Figure 4. ARS Bleaching evolution during the postdischarge.

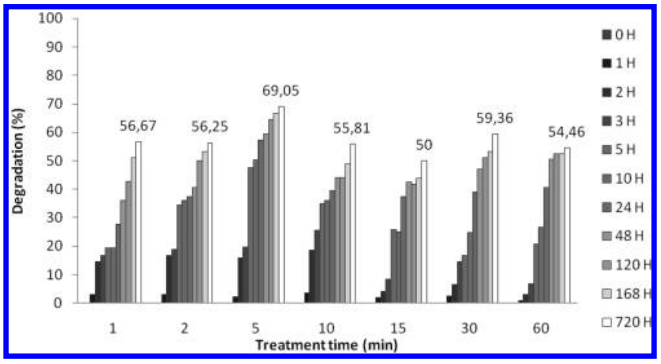

Figure 5. ARS COD abatement during the postdischarge.

species (i.e., peroxynitrite) directly correlated with the quantity of organic solute to be degraded. For short exposures, the concentration of $ONOO^-$ increases with t^*, before the degradation kinetics becomes significant. This means that a system of opposite reactions takes place involving the incorporation of peroxynitrite and its disappearance through its reaction with the solute. The occurrence of a maximum in the pollutant abatement as a function of t_{TPDR} for given t^* and pollutant concentration introduces the idea of dose as a function of waste concentration and exposure time which is otherwise suggested by microbial inactivation by glidarc process.

Peroxynitrite (peroxynitrous acid) is formed in the presence of hydrogen peroxide and nitrous acid (reactions 26 and 27):

$$H_2O_2 + HNO_2 \rightarrow ONOOH + H_2O \quad (26)$$

$$ONOOH + OH^- \rightarrow ONOO^- + H_2O \quad (27)$$

Both of HNO_2 and H_2O_2 are considered strong oxidizing agents, with redox potentials of ($E^\circ(HNO_2/^\bullet NO)$ = 0.983 V/SHE; $E^\circ(HNO_2/N_2O)$ = 1.297 V/SHE; $E^\circ(H_2O_2/H_2O)$ = 1.776 V/SHE).[33]

In treated solution, H_2O_2 is formed by recombination of hydroperoxyls and hydroxyls radicals (reactions 29 and 30). It usually occurs in slows reactions.[35]

$$H^\bullet + O_2 \rightarrow HO_2^\bullet \quad (28)$$

$$HO_2^\bullet + HO_2^\bullet \rightarrow H_2O_2 + O_2 \quad (29)$$

$$^\bullet OH + ^\bullet OH \rightarrow H_2O_2 \quad (30)$$

while nitrous acid is produced due to $^\bullet NO$ diffusion at the beginning of treatment. According to literature[57,58] H_2O_2, NO, and their derivates as peroxynitrite are responsible of postdischarge phenomena. Some authors[59] suggest that the formation of peroxynitrous acid and peroxynitrite may be related to the synergetic effect of acidified nitrites by H_2O_2 and nitrates.

Peroxynitrite may be formed according to Figure 6 from humid air as plasma gas. An applied electric discharge to humid

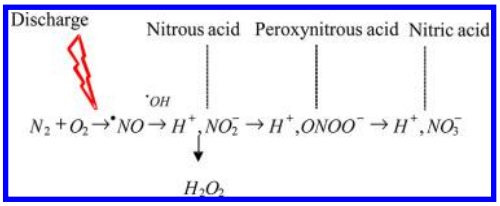

Figure 6. Peroxynitrite plasma humid air formation.

air generates initially $^\bullet NO$ and $^\bullet OH$ which subsequently form nitrous acid. The reaction of HNO_2 with H_2O_2 results in peroxynitrite which isomerizes to give nitric acid.

$$ONOOH \rightarrow HNO_3 \quad (31)$$

Peroxynitrous, nitrous, and nitric acid can be formed in different ways due to the large number of reactive species present in plasma humid air.

3.3. Kinetics Study. The bleaching kinetics of ARS were studied using zero-, first-, and second-order reaction kinetics. The statistical data calculation was based within the reaction period from 0 to 48 h. The expressions were presented as below (eqs 32−34):

Zero-order reaction kinetics:

$$\frac{dC}{dt_{TPDR}} = -k_0 \quad (32)$$

First-order reaction kinetics:

$$\frac{dC}{dt_{TPDR}} = -k_1 C \quad (33)$$

Second-order reaction kinetics:

$$\frac{dC}{dt_{TPDR}} = -k_2 C^2 \quad (34)$$

where C is the concentration of ARS; k_0, k_1, and k_2 represent the apparent kinetic rate constants of zero-, first- and second-order reaction kinetics, respectively; t is the postdischarge time.

Integrating the eqs 32−34 leads to the following equation:

dx.doi.org/10.1021/ie302964a | Ind. Eng. Chem. Res. 2013, 52, 1471−1480

$$\frac{C_0}{C} = k_0 t_{TPDR} \quad (35)$$

$$\ln\left(\frac{C_0}{C}\right) = k_1 t_{TPDR} \quad (36)$$

$$\frac{1}{C} - \frac{1}{C_0} = k_2 t_{TPDR} \quad (37)$$

The linearized expressions are given by eqs 35−37 were used to draw Figures 7 panels a, b, and c which show the relationship between C_0/C, $\ln(C_0/C)$, and $1/C - 1/C_0$ and postdischarge time.

The slopes of the kinetic plots were used to determine the rate constants k_0, k_1, and k_2 whose values are given in Table 4 with the corresponding regression coefficients.

Results show that the bleaching of the ARS samples treated by discharge at t^*: 0, 1, 2, 5, 15, 30, and 60 min followed the second order kinetics with respect to dye concentration. The concentration is in the same order as the oxidizing species, which leads to eq 38 and eq 39.

$$-\frac{d[ARS]}{dt_{TPDR}} = k_2[ARS][^{\bullet}OH] \quad (38)$$

$$-\frac{d[ARS]}{dt_{TPDR}} = k_2[ARS]^2 \quad (39)$$

The results obtained for the samples treated during 1, 5, and 15 min and exposed to the postdischarge at t_{TPDR} of 1, 3, 5, 10, 24, and 48 h (Figure 7) show an exponential curve.

The average regression coefficients have also been reported in Table 3 for comparison. The values are 0.8543, 0.9531, and 0.9895 for zero-, first-, and second order kinetics, respectively. The table indicates that the pseudo-second order reaction kinetics is justified.

It can be concluded that the bleaching of ARS by glidarc postdischarge fits the second-order reaction kinetic of the type

$$-r_{[ARS]} = k_1[ARS]^2 \quad (40)$$

The evolution of the rate constants indicates that the maximum value is 5.11×10^2 M^{-1} h^{-1} corresponding to t^* = 5 min of glidarc discharge treatment. Beyond this time, the value of k_2 decreases at 172.4 M^{-1} h^{-1}, for t^* = 60 min.

As shown in several papers, dye removal kinetics of most dyes by advanced oxidation processes can be evaluated using a pseudo-first-order rate model,[3,21,25,26] although in some papers a pseudo-second-order rate model was employed.[60−62]

S.P Sun et al. show that the decolorization kinetics of Orange G by the Fenton oxidation process followed the second-order reaction kinetics.[60] The apparent kinetic rate constants were found to be in the range of 2.66×10^2 to 3.4×10^4 min^{-1} $M^{-1.}$

Massakul Pukdee-Asa et al.[61] studied the degradation of three azo dyes. (CI Reactive Black 5, CI Reactive Orange 16, and CI Reactive Blue 2) by the fluidized-bed Fenton process. The apparent-second-order rate constants were calculated and varied from 0.7×10^2 to 30.1×10^2 $(mg/L)^{-1}$ (min^{-1}). Dye treatment using advanced oxidation processes with Co^{2+}/H_2O_2 and Co^{2+}/peroxymonosulfate (PMS) systems were investigated.[62] The degradation of Acid Red 183 follows the second-order kinetics.

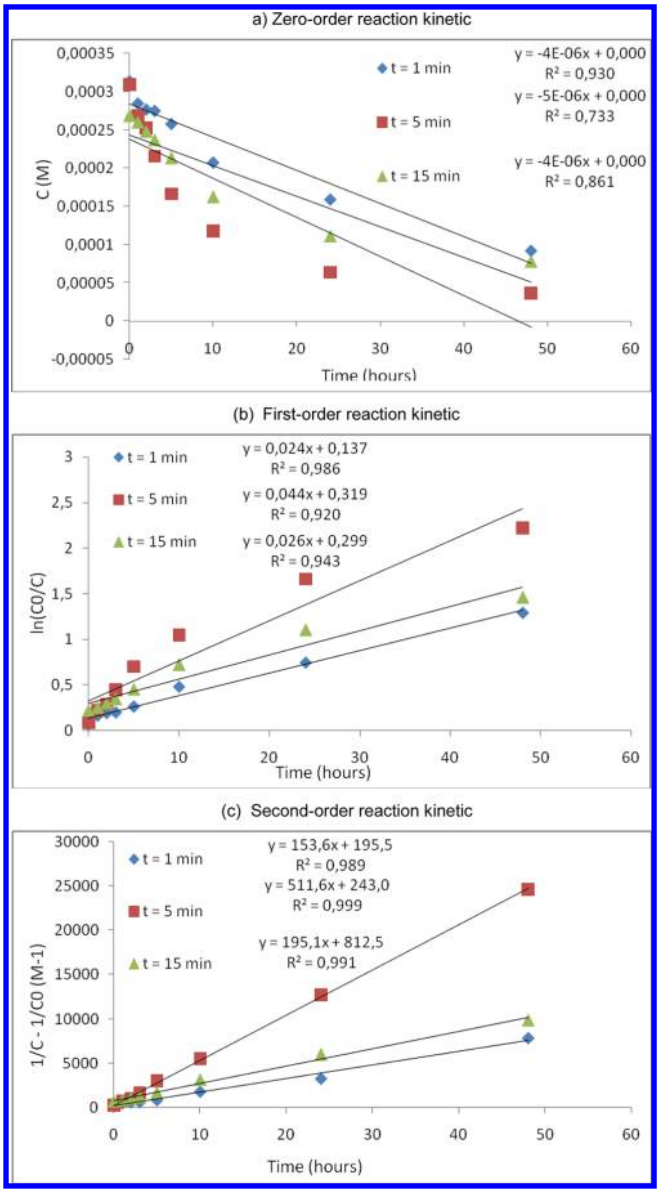

Figure 7. Zero- (a), first- (b), and second-order (c) kinetics rate constants for the bleaching of ARS: treated by discharge t^*= 1, 5, and 15 min, treated by postdischarge t_{TPDR} = 0−48 h.

3.4. Comparative Study of ARS Different Treatment Methods. The efficiency and processing time are the basic criteria for the choice of adequate treatment because it is a question of time and energy economy.[63] Table 5 shows the bleaching rates of ARS treated by several different methods, included ARS concentration and bleaching time maximum. We can note that plasma treatment and postdischarge increase the discoloration rates of ARS after a very short plasma treatment time despite relatively high ARS concentration. One of most plasma glidarc treatment problems is energy consumption; this is why an energy meter measuring electrical power is disposed in plasma installation. Energy consumption is evaluated to be 0.4 kWh.[34]

Our study reveals a higher bleaching (and degradation) rate after 5 min of electric discharge corresponding to 0.03 kWh of energy consumption. Technical cost evaluation takes into account the reagents used and electricity consumption.[64] In our case, no chemical product is added during plasma glidarc treatment and its postdischarge phenomena is very attractive.

dx.doi.org/10.1021/ie302964a | Ind. Eng. Chem. Res. 2013, 52, 1471−1480

Table 4. The Zero-, First-, and Second-Order Kinetics Rate Constants for the Bleaching of ARS Treated by Postdischarge

	postdischarge time, t_{TPDR}, 0−48 h					
	zero-order (M h^{-1})		first-order (h^{-1})		second-order (M^{-1} h^{-1})	
t^* (min)	K_0	R^2	K_1	R^2	K_2	R^2
1	4.35×10^{-6}	0.9306	0.0246	0.9869	1.53×10^{2}	0.9894
2	5.42×10^{-6}	0.9076	0.0397	0.9876	3.73×10^{2}	0.9804
5	5.12×10^{-6}	0.7337	0.0441	0.9208	5.11×10^{2}	0.9996
10	4.90×10^{-6}	0.763	0.0432	0.9131	4.98×10^{2}	0.9877
15	4.01×10^{-6}	0.861	0.0265	0.9435	1.95×10^{2}	0.9917
30	2.96×10^{-6}	0.8841	0.0226	0.9588	1.87×10^{2}	0.9963
60	2.44×10^{-6}	0.9007	0.0198	0.9616	1.72×10^{2}	0.9814

Table 5. ARS Bleaching Rates Treated by Different Methods

methods	ARS concentration (mg L^{-1})	% bleaching	treatment time (min)
DBD discharge	100[20]	100	40
glow plasma discharge	30[17]	63.3	40
catalyst biomimetic process	104.5[8]	100	180
present study: direct discharge	114	7/42.1	5/60
postdischarge	114	82.1 (t_{TPDR} = 0−48 h)	5

4. CONCLUSIONS

The detailed study of the behavior of an anthraquinonic dye (ARS) exposed to a gliding arc discharge is confirmed with a scarcely considered example: the activity of discharges burning in air over aqueous solutions and bleaching and degradation of the targeted dye. The bleaching mechanism is a complex process which verifies pseudo-second-order reaction ($k_2 = 3 \times 10^2$ M^{-1} h^{-1}), that is, a feature which has not been identified up to now. Complementary experiments performed in the presence or the absence of incorporated sulphamic acid known for its ability to inhibit the formation of nitrite ions and therefore of their derivatives, support the assumption that nitrite and peroxynitrite ions are the key agents of the degradation process.

Additionally, postdischarge evolution of the plasma-treated solution was successfully investigated. TPDR already identified in the degradation process of various organic solutes were also evidenced in that of ARS and observed for postdischarge times t_{TPDR} longer than a week, which is unusual. A detailed investigation underlined the influence of the preliminary exposure time t^* before TPDR develop and led to the conclusion that the postdischarge treatment effects presented a maximum both for bleaching and degradation for short exposure times t^*. An explanation is proposed in connection with the concept of dose which depends on the pollutant concentration: a given quantity of waste solute requires a suitable quantity of formed peroxynitrite for its oxidizing degradation; the number of formed peroxynitrite species is related to the burning time t^* of the arc discharge (and hence to the quantity of NO formed in given electrical conditions).

This feature is of major importance in industrial application for economy reasons, since the glidarc treatment then requires only few minutes exposure to reach complete pollutant abatement. Incidentally, it can also be underlined that the gliding arc is probably among the most efficient discharges burning at atmospheric pressure, mainly because it enables the formation of NO and of derivatives such as the strong oxidizing peroxynitrite species.

AUTHOR INFORMATION

Corresponding Author

*E-mail: f.abdelmalek@univ-mosta.dz. Address: BP 188, University of Mostaganem, Algeria.

Notes

The authors declare no competing financial interest.

ACKNOWLEDGMENTS

The authors thank the Algerian National Administration of Scientific Research (DG-RSDT) for financial support.

REFERENCES

(1) Ahmadi, M. F.; Bensalah, N.; Gadri, A. Electrochemical degradation of anthraquinone dye Alizarin Red S by anodic oxidation on boron-doped diamond. *Dyes Pigm.* **2007**, *73*, 86−89.

(2) Ghodbane, H.; Hamdaoui, O. Intensification of sonochemical decolorization of anthraquinonic dye Acid Blue 25 using carbon tetrachloride. *Ultrason. Sonochem.* **2009**, *16*, 455−461.

(3) Bouzaida, I.; Ferronato, C.; Chovelon, J. M.; Rammah, M. E.; Herrmann, J. M. Heterogeneous photocatalytic degradation of the anthraquinonic dye, Acid Blue 25 (AB25): A kinetic approach. *J. Photochem. Photobiol., A* **2004**, *168*, 23−30.

(4) Zucca, P.; Vinci, C.; Sollai, F.; Rescigno, A.; Sanjust, E. Degradation of Alizarin Red S under mild experimental conditions by immobilized 5,10,15,20-tetrakis (4-sulfonatophenyl) porphine−Mn-(III) as a biomimetic peroxidase-like catalyst. *J. Mol. Catal A: Chem.* **2008**, *288*, 97−102.

(5) Galindo, C.; Jacques, P.; Kalt, A. Photooxidation of the phenylazonaphthol AO20 on TiO_2: Kinetic and mechanistic investigation. *Chemosphere* **2001**, *45*, 997.

(6) Ao, C. H.; Leung, M. K. H.; Lam, R. C. W.; Leung, D. Y. C.; Vrijmoed, L. L. P.; Yam, W. C.; Ng, S. P. Photocatalytic decolorization of anthraquinonic dye by TiO_2 thin film under UVA and visible-light irradiation. *Chem. Eng. J.* **2007**, *129*, 153−159.

(7) Ghezzar, M. R.; Abdelmalek, F.; Belhadj, M.; Benderdouche, N.; Addou, A. Gliding arc plasma assisted photocatalytic degradation of anthraquinonic acid green 25 in solution with TiO_2. *Appl. Catal. B: Environ.* **2007**, *72*, 304−313.

(8) Fabbri, D.; Calza, P.; Prevot, A. B. Photoinduced transformations of Acid Violet 7 and Acid Green 25 in the presence of TiO_2 suspension. *J. Photochem. Photobiol., A* **2010**, *213*, 14−22.

(9) Pozdnyakova, N. N.; Rodakiewicz-Nowak, J.; Turkovskaya, O. V.; Haber, J. Oxidative degradation of polyaromatic hydrocarbons and their derivatives. Catalyzed directly by the yellow laccase from *Pleurotus ostreatus* D1. *Jo. Mol. Catal. B* **2006**, *41*, 8−15.

(10) Puchtler, H.; Meloan, S. N.; Terry, M. S. On the history and mechanism of alizarin and alizarin red S stains for calcium. *J. Histochem. Cytochem.* **1969**, *17* (2), 110−124.

(11) Turcanu, A.; Bechtold, T. pH dependent redox behaviour of Alizarin Red S (1,2-dihydroxy-9,10-anthraquinone-3-sulfonate)—Cyclic voltammetry in presence of dispersed vat dye. *Dyes Pigm.* **2011**, *91*, 324−331.
(12) Vandevivere, P. C.; Bianchi, R.; Verstraete, W. Treatment and reuse of wastewater from the textile wet-processing industry: Review of emerging technologies. *J. Chem. Technol. Biotechnol.* **1998**, *72*, 289−302.
(13) Konstantinou, I. K.; Albanis, T. A. TiO_2-assisted photocatalytic degradation of azo dyes in aqueous solution: Kinetic and mechanistic investigations: A review. *Appl Catal B: Environ.* **2004**, *49* (1), 1−14.
(14) Panizza, M.; Cerisola, G. Electro-Fenton degradation of synthetic dyes. *Water Res.*. **2009**, *43*, 339−344.
(15) Marco Panizza, M.; Oturan, M. A. Degradation of Alizarin Red by electro-Fenton process using a graphite-felt cathode. *Electrochim. Acta* **2011**, *56*, 7084−7087.
(16) Gomathi Devi, L.; Rajashekhar, K. E.; Anantha Raju, K. S.; Girish Kumar, S. Kinetic modeling based on the non-linear regression analysis for the degradation of Alizarin Red S by advanced photo-Fenton process using zero valent metallic iron as the catalyst. *J. Mol. Catal. A* **2009**, *314*, 88−94.
(17) Gao, J. Z.; Yu, J.; Lu, Q.; He, X.; Yang, W.; Li, Y.; Pu, L.; Yang, Z.. Decoloration of Alizarin Red S in aqueous solution by glow discharge electrolysis. *Dyes Pigm.* **2008**, *76*, 47−52.
(18) Magureanu, M.; Piroi, D.; Gherendi, F.; Mandache, N. B.; Parvulescu, V. I. Decomposition of Methylene Blue in water by corona discharges. *Plasma Chem. Plasma Process.* **2008**, *28* (6), 677−688.
(19) Wen, Y. Z.; Liu, H. J.; Liu, W. P.; Jiang, X. Z. Degradation of organic contaminants in water by pulsed corona discharge. *Plasma Chem. Plasma Process.* **2005**, *25* (2), 137−146.
(20) Xue, J.; Chen, L.; Wang, H. Degradation mechanism of Alizarin Red in hybrid gas−liquid phase dielectric barrier discharge plasmas: Experimental and theoretical examination. *Chem. Eng. J.* **2008**, *138*, 120−127.
(21) Abdelmalek, F.; Benstaali, B.; Brisset, J. L.; Addou, A. Plasmadegradation of dyes orange II and malachite green in water by gliding arc. *Orient. J. Chem.* **2005**, *21*, 21−24.
(22) Abdelmalek, F.; Gharbi, S.; Benstaali, B.; Addou, A.; Brisset, J. L. Plasmachemical degradation of azo dyes by humid air plasma: Yellow Supranol 4 GL, Scarlet Red Nylosan F3 GL and industrial waste. *Water Res.* **2004**, *38*, 2339.
(23) Abdelmalek, F.; Ghezzar, M. R.; Belhadj, M.; Addou, A.; Brisset, J. L. Bleaching and degradation of textile dyes by nonthermal plasma process at atmospheric pressure. *Ind. Eng. Chem. Res.* **2006**, *45*, 23−29.
(24) Benstaali, B.; Bastaki, N.; Addou, A.; Brisset, J. L. Plasmachemical and photocatalytic degradation of methylorange. *Int J. Environ. Waste Manage.* **2012**, in press.
(25) Doubla, A.; Bouba Bello, L.; Fotso, M.; Brisset, J. L. Plasmachemical decolourisation of bromothymol blue by gliding arc discharge. *Dyes Pigm.* **2008**, *77*, 118−124.
(26) Merouani, D. R.; Abdelmalek, F.; Taleb, F.; Martel, M.; Semmoud, A.; Addou, A. Plasma treatment by gliding arc discharge of dyes/dye mixtures in the presence of inorganic salts. *Arab. J. Chem.* **2011**, DOI: 10.1016/j.arabjc.2011.01.034.
(27) Marouf-Khelifa, K.; Abdelmalek, F.; Khelifa, A.; Addou, A. TiO_2-assisted degradation of a perfluorinated surfactant in aqueous solutions treated by gliding arc discharge. *Chemosphere.* **2008**, *70*, 1995−2001.
(28) Ghezzar, M. R.; Abdelmalek, F.; Belhadj, M.; Benderdouche, N.; Addou, A. Enhancement of the bleaching and degradation of textile wastewaters by Gliding arc discharge plasma in the presence of TiO_2 catalyst. *J. Hazard. Mater.* **2009**, *164*, 1266−1274.
(29) Njoyim-Tamungang, E.; Laminsi, S.; Ghogomu, P.; Njopwouo, D.; Brisset, J. L. Pollution control of surface waters by coupling gliding discharge treatment with incorporated oyster shell powder. *Chem. Eng. J.* **2011**, *173*, 303−308.
(30) Tsagou-Sobze, E. B.; Moussa, D.; Doubla, A.; Hnatiuc, E.; Brisset, J. L. Gliding discharge induced oxidation of a toxic alkaloid. *J. Hazard. Mater.* **2008**, *152*, 446−449.
(31) Moussa, D.; Brisset, J. L. Disposal of spent tributylphosphate by gliding arc plasma. *J. Hazard. Mater.* **2003**, *102* (2−3), 189−200.
(32) Moussa, D.; Brisset, J. L.; Hnatiuc, E.; Decobert, G. Plasmachemical destruction of triaurylamine from nuclear laboratory reprocessing plants. *Ind. Eng. Chem. Res.* **2006**, *45*, 23−29.
(33) Yan, J-h.; Du, C-m., Li, X-d; Sun, X-d; Ni, M-j.; Cen, K-f.; Cheron, B. Plasma chemical degradation of phenol in solution by gas−liquid gliding arc discharge. *Plasma Sources Sci. Technol.* **2005**, *14*, 637−644.
(34) Abdelmalek, F.; Torres, R. A.; Combet, E.; Petrier, C.; Pulgarin, C.; Addou, A. Gliding arc discharge (GAD) assisted catalytic degradation of bisphenol A in solution with ferrous ions. *Sep. Purif. Technol.* **2008**, *63*, 30−37.
(35) Moussa, D.; Doubla, A.; Kamgang Youbi, G.; Brisset, J.-L. Post discharge long life reactive intermediate involved in the plasmachemical degradation of an azoic dye. *IEEE Trans. Plasma Sci.* **2007**, *35*, 444−451.
(36) Doubla, A.; Abdelmalek, F.; Khelifa, K.; Addou, A.; Brisset, J.-L. Post discharge plasma-chemical oxidation of iron (II) complexes. *J. Appl. Electrochem.* **2003**, *33*, 73−77.
(37) Doubla, A.; Brisset, J.-L. Post-discharge kinetics associated with a plasma-chemical nucleophilic substitution and application to the analysis of plasma activated CO. *J. Appl. Electrochem.* **2006**, *36*, 77−85.
(38) Kamgang Youbi, G.; Herry, J.-M.; Bellon-Fontaine, M.-N.; Brisset, J.-L.; Doubla, A.; Naïtali, M. Evidence of the temporal post-discharge decontamination of bacteria by gliding electric discharges: Application to *Hafnia alvei*. *Appl. Environ. Microbiol.* **2007**, *73*, 4791−4796.
(39) Brisset, J.-L.; Benstaali, B.; Moussa, D.; Fanmoe, J.; Njoyim-Tamungang, E. Acidity control of plasma-chemical oxidation: Applications to dye removal, urban waste abatement and microbial inactivation. *Plasma Sources Sci. Technol.* **2011**, *20*, 034021 DOI: 10.1088/0963-0252/20/3/034021.
(40) Njoyim-Tamungang, E.; Ghogomu, P.; Laminsi, S.; Nzali, S.; Doubla, A.; Brisset, J.-L. Coupling gliding discharge treatment and catalysis by oyster shell powder for pollution abatement of surface waters. *Ind. Eng. Chem. Res.* **2009**, *48*, 9773−9780.
(41) Brisset, J.-L.; Benstaali, B.; Moussa, D. ; Fanmoe, J. ; Njoyim-Tamungang, E. Acidity control of plasma chemical oxidizing treatments of organic wastes. *Plasma Sources Sci. Technol.* **2011**. Special issue 20: 034021.
(42) Lesueur, H. ; Czernichowski, A. ; Chapelle, J. ; Dispositif de génération de plasma basse température par formation de décharges électriques glissantes. (A device for generating a low temperature plasma by means of gliding electrical discharges). French Patent. 1988, 88−2,639,172.
(43) Czernichowski, A. *Gliding Discharge Reactor for H_2S Valorization or Destruction in Non-thermal Plasma Techniques for Pollution Control*; Penetrante, B. M., Shultheis, S. E., Eds.; NATO ASI Series G, Vol. *34*, Part B; Springer-Verlag: Berlin, 1993; pp 371−387.
(44) Benstaali, B.; Boubert, P.; Cheron, B. G.; Addou, A.; Brisset, J.-L. Density and rotational temperature measurements of the NO and OH radicals produced by a gliding arc in humid air and their interaction with aqueous solutions. *Plasma Chem. Plasma Process.* **2002**, *22*, 553−571.
(45) Gonzalez, M. C.; Braun, A. M. VUV photolysis of aqueous solutions of nitrate and nitrite. *Res. Chem. Intermed.* **1995**, *21* (8/9), 837−859.
(46) *NFT 90-102: la Qualité de l'Eau, Tome II*; AFNOR: Saint-Denis Cedex, France, 1999.
(47) Moussa, D.; Abdelmalek, F.; Benstaali, B.; Addou, A.; Hnatiuc, E.; Brisset, J.-L. Acidity control of the oxidation reactions induced by nonthermal plasma treatment of aqueous effluents in pollutant abatement processes. *Eur. Phys. J.-Appl. Phys.* **2005**, *29*, 189−199.
(48) Brisset, J.-L.; Hnatiuc, E. Peroxynitrite: A re-examination of the chemical properties of nonthermal discharges burning in air over aqueous solutions. *Plasma Chem. Plasma Process.* **2012**, *32*, 655−674.

(49) Poplin, M. Removal of aqueous pollutants with gliding arc discharge. BS Honors Thesis, Chemical and Biomedical Engineering, Florida State University, Tallahassee, FL, USA. 2006
(50) Burlica, R.; Locke, B. R. Pulsed plasma gliding-arc discharges with water spray. *IEEE Trans. Ind. Appl.* **2008**, *44* (2), 83−89.
(51) Burlica, R.; Kirkpatrick, M. J.; Locke, B. R. Formation of reactive species in gliding arc discharges with liquid water. *J. Electrostat..* **2006**, *64*, 35−43.
(52) Logager, T.; Sehested, K. Formation and decay of peroxynitrous acid: A pulse radiolysis study. *J. Phys. Chem.* **1993**, *97* (25), 6664−6669.
(53) Grätzel, M.; Henglein, A.; Taniguchi, S. Pulsradiolytische Beobachtungen¨uber die reduktion des nitrat ions und¨uber bildung und zerfall der persalpetrigen saeure in ẅassriger lösung, Ber. Bunsenges. *Phys. Chem.* **1970**, *74*, 292−298.
(54) Marouf-Khelifa, K.; Abdelmalek, F.; Khelifa, A.; Belhadj, M.; Addou, A.; Brisset, J.-L. Reduction of nitrite by sulfamic acid and sodium azide from aqueous solution treated by gliding arc discharge. *Sep. Purif. Technol.* **2006**, *50*, 373−379.
(55) Iya-Sou, D.; Ognier, S. ; Laminsi, S. ; Cavadias, S. Specific role of active species created by gliding arc discharge for removal of persistent organic pollutants in aqueous solution: Elimination mechanism. The 20th International Symposium on Plasma Chemistry; Philadelphia, USA, July 24−29, 2011.
(56) Brisset, J.-L.; Moussa, D.; Doubla, A.; Hnatiuc, E.; Hnatiuc, B.; Kamgang Youbi, G.; Herry, J.-M.; Naïtali, M.; Bellon-Fontaine, M.-N. Chemical reactivity of discharges and temporal post-discharges in plasma treatment of aqueous media: Examples of gliding discharge treated solutions. *Ind. Eng. Chem. Res.* **2008**, *47*, 5761−5781.
(57) Miyahara, T.; Ochiai, S.; Sato, T. Interaction mechanism between a post-discharge flow and water surface. *Eur. Phys. Lett..* **2009**, *86*, 4500 DOI: 10.1209/0295-5075/86/45001.
(58) Traylor, M. J.; Pavlovich, M. J.; Karim, S.; Hait, P.; Sakiyama, Y.; Clark, D. S.; Graves, D. B. Long-term antibacterial efficacy of air plasma-activated water. *J. Phys. D: Appl. Phys.* **2011**, 44472001 DOI: 10.1088/0022-3727/44/47/472001.
(59) Naïtali, M.; Kamgang-Youbi, G.; Herry, J.-M.; Bellon-Fontaine, M.-N.; Brisset, J.-L. Combined effects of long-living chemical species during microbial inactivation using atmospheric plasma-treated water. *Appl. Environ. Microbiol.* **2010**, *76*, 7662−7664, DOI: 10.1128/AEM.01615-10.
(60) Sun, S.-P.; Li, C.-J.; Sun, J.-H.; Shi, S.-H.; Fan, M.-H.; Zhou, Q. Decolorization of an azo dye Orange G in aqueous solution by Fenton oxidation process: Effect of system parameters and kinetic study. *J. Hazard. Mater.* **2009**, *161*, 1052−1057.
(61) Pukdee-Asa, M.; Su, C.-C.; Ratanatamskul, C.; Lub, M.-C. Degradation of azo dye by the fluidised-bed Fenton process. *Color. Technol.* **2011**, 28 DOI: 10.1111/j.1478-4408.2011.00325.x.
(62) Ling, S. K.; Wang, S.; Peng, Y. Oxidative degradation of dyes in water using Co^{2+}/H_2O_2 and Co^{2+}/peroxymonosulfate. *J. Hazard. Mater.* **2010**, *178*, 385−389.
(63) Zhou, X.-J.; Guo, W.-Q.; Yang, S.-S.; Ren, N.-Q. A rapid and low energy consumption method to decolorize the high concentration triphenylmethane dye wastewater: Operational parameters optimization for the ultrasonic-assisted ozone oxidation process. *Bioresour. Technol.* **2012**, *105*, 40−47.
(64) Chang, S.-H.; Chuang, S.-H.; Li, H.-C.; Liang, H.-H.; Huang, L.-C. Comparative study on the degradation of I.C. Remazol Brilliant Blue R and I.C. Acid Black 1 by Fenton oxidation and Fe_0/air process and toxicity evaluation. *J. Hazard. Mater.* **2009**, *166*, 1279−1288.